pH-Induced Deswelling Kinetics of Sterically Stabilized Poly(2-vinylpyridine) Microgels Probed by Stopped-Flow Light Scattering

Jun Yin,[†] Damien Dupin,[‡] Junfang Li,[†] Steven P. Armes,*[,‡] and Shiyong Liu*[,†]

Key Laboratory of Soft Matter Chemistry, Department of Polymer Science and Engineering, Hefei National Laboratory for Physical Sciences at the Microscale, University of Science and Technology of China, Hefei, Anhui 230026, China, and Department of Chemistry, University of Sheffield, Brook Hill, Sheffield, South Yorkshire, S3 7HF, United Kingdom

Received May 8, 2008. Revised Manuscript Received June 12, 2008

Near-monodisperse, sterically stabilized poly(2-vinylpyridine) (P2VP) microgels were synthesized by emulsion polymerization. These particles exhibited completely reversible pH-responsive swelling/deswelling behavior in aqueous solution. Stopped-flow light scattering was employed to investigate the kinetics of pH-induced deswelling in highly dilute dispersions. Upon a pH jump from 2 to various final solution pH values (≥5.4), the scattered light intensity of an aqueous dispersion of a 1960 nm microgel exhibited an abrupt initial increase, followed by a gradual decrease to the final equilibrium value. The whole microgel-to-latex deswelling process occurred over time scales of ∼0.5−1.0 s, which is much slower than the kinetics for latex-to-microgel swelling. The microgel deswelling kinetics depends on the final pH, with a higher final pH leading to a faster rate of shrinkage. Close inspection of the deswelling kinetics during the early stages (<0.2 s) revealed that initial microgel collapse occurred within ∼50 ms, with more rapid transitions being observed when higher final pH values were targeted. Addition of external salt significantly accelerates the kinetics of deswelling. Systematic studies of the microgel-to-latex transition for a series of six near-monodisperse P2VP particles (with swollen microgel diameters ranging from 1270 to 4230 nm) has also been investigated. The characteristic deswelling time for initial microgel collapse, $\tau_{deswell}$, correlated fairly well with the initial swollen microgel radius, R, in agreement with the Tanaka equation. Moreover, the collective diffusion coefficient of the gel network, D, calculated from the slope of the $\tau_{deswell}-R^2$ curve, was of the order of 10^{-7} cm^2 s^{-1}.

Introduction

Microgel particles are cross-linked latex particles which can swell appreciably in a good solvent and are typically dispersed in water. Compared to macroscopic gels, microgels exhibit much faster rates of (de)swelling in response to external stimuli such as pH,[1–11] temperature,[10,12–18] and ionic strength.[17,19–21] This appears to be particularly advantageous for practical applications, such as drug delivery,[22,23] controlled release,[24,25] catalysis,[26,27] and chemical separation.[28,29] The pH-responsive character and volume phase transitions (VPT) exhibited by microgels usually arise from changes in osmotic pressure and/or charge density.[30] Various pH-responsive microgels have been reported over the past few decades, such as lightly cross-linked alkali-swellable latexes containing methacrylic acid (MAA) residues,[10,31,32] *N*-isopropylacrylamide-based multiresponsive copolymer microgels containing either acidic or basic comonomers,[33–35] and

* To whom correspondence should be addressed. Email: sliu@ustc.edu.cn (S.L.); s.p.armes@sheffield.ac.uk (S.P.A.).
† University of Science and Technology of China.
‡ University of Sheffield.

(1) Morris, G. E.; Vincent, B.; Snowden, M. J. *J. Colloid Interface Sci.* **1997**, *190*, 198–205.
(2) Chiu, H. C.; Lin, Y. F.; Hung, S. H. *Macromolecules* **2002**, *35*, 5235–5242.
(3) Dupin, D.; Rosselgong, J.; Armes, S. P.; Routh, A. *Langmuir* **2007**, *23*, 4035–4041.
(4) Dupin, D.; Fujii, S.; Armes, S. P.; Reeve, P.; Baxter, S. M. *Langmuir* **2006**, *22*, 3381–3387.
(5) Dai, Z.; Yang, X. L.; Huang, W. Q. *Polym. Int.* **2007**, *56*, 224–230.
(6) Xiang, Y. Q.; Zhang, Y.; Chen, D. J. *Polym. Int.* **2006**, *55*, 1407–1412.
(7) Pich, A.; Tessier, A.; Boyko, V.; Lu, Y.; Adler, H. J. P. *Macromolecules* **2006**, *39*, 7701–7707.
(8) Bromberg, L.; Temchenko, M.; Alakhov, V.; Hatton, T. A. *Langmuir* **2005**, *21*, 1590–1598.
(9) Hoare, T.; Pelton, R. *Langmuir* **2006**, *22*, 7342–7350.
(10) Robinson, D. N.; Peppas, N. A. *Macromolecules* **2002**, *35*, 3668–3674.
(11) Amalvy, J. I.; Wanless, E. J.; Li, Y.; Michailidou, V.; Armes, S. P.; Duccini, Y. *Langmuir* **2004**, *20*, 8992–8999.
(12) Wang, J. P.; Gan, D. J.; Lyon, L. A.; El-Sayed, M. A. *J. Am. Chem. Soc.* **2001**, *123*, 11284–11289.
(13) Pelton, R. *Adv. Colloid Interface Sci.* **2000**, *85*, 1–33.
(14) Saunders, B. R.; Vincent, B. *Adv. Colloid Interface Sci.* **1999**, *80*, 1–25.
(15) Hassan, C. M.; Doyle, F. J.; Peppas, N. A. *Macromolecules* **1997**, *30*, 6166–6173.
(16) Klier, J.; Scranton, A. B.; Peppas, N. A. *Macromolecules* **1990**, *23*, 4944–4949.
(17) Cheng, H.; Wu, C.; Winnik, M. A. *Macromolecules* **2004**, *37*, 5127–5129.
(18) Sugiyama, M.; Annaka, M.; Hara, K. *J. Phys. Soc. Jpn.* **2002**, *71*, 1035–1038.
(19) Hampton, K. W.; Ford, W. T. *Macromolecules* **2000**, *33*, 7292–7299.
(20) Mohan, Y. M.; Dickson, J. P.; Geckeler, K. E. *Polym. Int.* **2007**, *56*, 175–185.
(21) Ngai, T.; Auweter, H.; Behrens, S. H. *Macromolecules* **2006**, *39*, 8171–8177.
(22) Ichikawa, H.; Fukumori, Y. *J. Controlled Release* **2000**, *63*, 107–119.
(23) Chen, G. H.; Hoffman, A. S. *Macromol. Rapid Commun.* **1995**, *16*, 175–182.
(24) Richter, A.; Turke, A.; Pich, A. *Adv. Mater.* **2007**, *19*, 1109–1112.
(25) Niu, J.; Shi, F.; Liu, Z.; Wang, Z.; Zhang, X. *Langmuir* **2007**, *23*, 6377–6384.
(26) Bergbreiter, D. E.; Case, B. L.; Liu, Y. S.; Caraway, J. W. *Macromolecules* **1998**, *31*, 6053–6062.
(27) Bergbreiter, D. E.; Liu, Y. S.; Osburn, P. L. *J. Am. Chem. Soc.* **1998**, *120*, 4250–4251.
(28) Kayaman, N.; Kazan, D.; Erarslan, A.; Okay, O.; Baysal, B. M. *J. Appl. Polym. Sci.* **1998**, *67*, 805–814.
(29) Umeno, D.; Kawasaki, M.; Maeda, M. *Bioconjugate Chem.* **1998**, *9*, 719–724.
(30) Plunkett, K. N.; Kraft, M. L.; Yu, Q.; Moore, J. S. *Macromolecules* **2003**, *36*, 3960–3966.
(31) Rodriguez, B. E.; Wolfe, M. S.; Fryd, M. *Macromolecules* **1994**, *27*, 6642–6647.
(32) Saunders, B. R.; Crowther, H. M.; Vincent, B. *Macromolecules* **1997**, *30*, 482–487.
(33) Bradley, M.; Ramos, J.; Vincent, B. *Langmuir* **2005**, *21*, 1209–1215.
(34) Gan, D. J.; Lyon, L. A. *J. Am. Chem. Soc.* **2001**, *123*, 7511–7517.
(35) Jones, C. D.; Lyon, L. A. *Macromolecules* **2003**, *36*, 1988–1993.

10.1021/la8014282 CCC: $40.75
Published on Web 07/22/2008

acid-swellable latexes based on either 4-vinylpyridine (4VP) or 2-vinylpyridine (2VP).[3,4,11,36,37]

In spite of its importance in both academic research and practical applications, the kinetics of the VPT for gels has not been fully understood yet. In principle, one could study the kinetics of the phase transition of a gel either on a macroscopic scale (by observing the change in the shape, size, and transient patterns) or on a microscopic scale (by observing the internal dynamic properties).[8,30,38–47] In 1979 Tanaka and Fillmore proposed that the rate of gel swelling is dominated by the motion of polymer network.[45] This motion, which occurs during swelling, was described by a collective diffusion coefficient, D. Here D is defined as the ratio of the osmotic bulk modulus, K, of the polymer network to the frictional coefficient, f, between the polymer network and solvent. They also proposed that the time required for a gel to change its volume and shape was proportional to the square of the characteristic length of the gel.

$$\tau = (\text{length})^2/(K/f) = (\text{length})^2/D \quad (1)$$

For the VPT of a spherical gel, the characteristic time is simply proportional to the square of its radius, R; hence $\tau = R^2/D$.

Tanaka and Fillmore[45] synthesized a series of spherical macrogels of polyacrylamide in paraffin oil with diameters ranging from 1 to 2.8 mm, and observed a linear relationship between the characteristic time, τ, and the square of the gel radius (R) during gel swelling in water. From the slope of the curve, they obtained $D = 3.2 \times 10^{-7}$ cm^2 s^{-1} for these spherical gels, which was close to that obtained from dynamic light scattering (DLS, 3.0×10^{-7} cm^2 s^{-1}). For swelling or deswelling of spherical poly(*N*-isopropylacrylamide) (PNIPAM) gels, the VPT exhibited critical kinetic behavior near the phase transition temperature, i.e., the transition required very long time scales. Moreover, the D value passed through a minimum if the VPT was restricted to the linear response region and gel volume change was small. Suárez et al.[48] recently synthesized PNIPAM minigels with different sizes in the micrometer range, in order to allow their swelling kinetics to be monitored by video optical microscopy. They estimated a D of 1.0×10^{-6} cm^2 s^{-1} for the swelling of these minigels, which lies between the self-diffusion coefficient of water (2.3×10^{-5} cm^2 s^{-1} at 25 °C), and the diffusion coefficient reported for macroscopic PNIPAM gels ($\sim 5 \times 10^{-7}$ cm^2 s^{-1}).[38,44]

If the VPT is discontinuous, i.e., involves a first-order transition, volumetric changes of up to 3 orders of magnitude can be observed for gel swelling or shrinking. Matsuo and Tanaka[40] and Shibayama et al.[43,49] reported that the VPT transition kinetics during gel swelling follows single-exponential behavior and can be explained by the Tanaka-Fillmore theory (eq 1). However, gel deswelling was more complicated.[40,41,49] Tanaka's group[40] observed a three-stage process for the shrinking of spherical PNIPAM gels for large temperature jumps across the critical phase transition temperatures. The gel retains its spherical shape during the first stage while it shrinks to ~70−90% of its initial radius, accompanied with the formation of a dense and solvent-impermeable surface layer. This was followed by a "plateau period" in which the gel temporarily stops shrinking. In the third stage, bubbles appear at the gel surface and shrinking resumes. Interestingly, it was found that the relaxation times for the initial gel shrinkage regime, the plateau regime, and the final shrinkage regime scaled linearly with $R^{1.6}$, where R is the gel radius. Apparently, the calculated collective diffusion coefficient (D) for the gel network varies at different stages of gel deswelling and is dependent on the network concentration.[40] Shibayama et al.[43,49] also reported that the rate of deswelling of PNIPAM gels was strongly retarded; however, they did not observe any evidence for the formation of a dense surface "shell" layer during this transition.

As described above, previous studies of the VPT kinetics mainly focused on macroscopic gels. In principle, the time needed for volume changes can be estimated to be 10^7 s for spherical macrogels of ~1 cm radius as D is usually on the order of 10^{-7} cm^2 s^{-1}, while it is only $\sim 10^{-1}$ s for spherical microgel particles with a radius of ~1 μm.[50] However, the latter time scale is sufficiently short to pose significant experimental difficulties for accurately monitoring the kinetics of (de)swelling of microgels, hence experimental data are relatively rare.[3,4,12,33,37]

Lyon and co-workers[12] prepared a series of PNIPAM-based core−shell microgels in which the sizes and cross-linking densities of their cores and shells were varied. They reported that temperature-induced (~10 °C jump, laser pulse) microgel deswelling occurred over a time scale of microseconds. However, they also deduced that such deswelling resulted in a relatively small reduction (<10%) of particle volume under their experimental setup, thus only a thin peripheral layer of the microgel particles was involved. This indicated that extensive deswelling did not occur. The main limitation in their experimental setup was that the temperature could only be maintained for a few milliseconds after the T-jump. Recently, Dupin and co-workers[3] studied the acid-induced swelling kinetics of a series of near-monodisperse sterically stabilized poly(2-vinylpyridine) (P2VP) latex particles with mean diameters ranging from 380 to 1010 nm, by using a stopped-flow apparatus equipped with a transmitted light (turbidimetric) detector. The characteristic swelling time for the latex-to-microgel transition was within the time scale of tens of milliseconds, which is in fairly good agreement with that predicted by the Tanaka equation.[45] A linear correlation was obtained between the characteristic swelling time, τ, and the square of the initial particle radius, R^2, prior to the pH jump. From the slope of the $\tau - R^2$ curve, the collective diffusion coefficient (D) can be calculated to be $\sim 1.5 \times 10^{-7}$ cm^2 s^{-1}.

To the best of our knowledge, the kinetics of microgel deswelling has not been reported yet. For macroscopic gels, it is already known that their multistage deswelling kinetics is drastically different to their swelling kinetics. Thus we were curious to examine whether microgel deswelling would also exhibit complex nonlinear behavior. Herein, we examined the kinetics of deswelling (i.e., the microgel-to-latex transition) using identical P2VP particles. The mean diameters of the initially swollen microgels ranged from 1270 to 4230 nm, as measured by dynamic light scattering (DLS) for an extremely dilute dispersion (4×10^{-6} g/mL). The same stopped-flow pH-jump technique was employed and time-resolved changes in the scattered light intensity were monitored using a more sensitive

(36) Ma, G. H.; Fukutomi, T. *Macromolecules* **1992**, *25*, 1870–1875.
(37) Loxley, A.; Vincent, B. *Colloid Polym. Sci.* **1997**, *275*, 1108–1114.
(38) Makino, K.; Hiyoshi, J.; Ohshima, H. *Colloids Surf., B* **2000**, *19*, 197.
(39) Matsuo, E. S.; Orkisz, M.; Sun, S. T.; Li, Y.; Tanaka, T. *Macromolecules* **1994**, *27*, 6791–6796.
(40) Matsuo, E. S.; Tanaka, T. *J. Chem. Phys.* **1988**, *89*, 1695–1703.
(41) Matsuo, E. S.; Tanaka, T. *Nature* **1992**, *358*, 482–485.
(42) Matsuo, E. S.; Tanaka, T. *Phase Trans.* **1994**, *46*, 217–228.
(43) Shibayama, M.; Nagai, K. *Macromolecules* **1999**, *32*, 7461–7468.
(44) Tanaka, T. *Phys. A* **1986**, *140*, 261.
(45) Tanaka, T.; Fillmore, D. J. *J. Chem. Phys.* **1979**, *70*, 1214–1218.
(46) Tanaka, T.; Sato, E.; Hirokawa, Y.; Hirotsu, S.; Peetermans, J. *Phys. Rev. Lett.* **1985**, *55*, 2455.
(47) Andersson, M.; Axelsson, A.; Zacchi, G. *J. Controlled Release* **1998**, *50*, 273–281.
(48) Suárez, I. J.; Fernandez-Nieves, A.; Marquez, M. *J. Phys. Chem. B.* **2006**, *110*, 25729–25733.
(49) Hirose, H.; Shibayama, M. *Macromolecules* **1998**, *31*, 5336–5342.
(50) Hirose, Y.; Amiya, T.; Hirokawa, Y.; Tanaka, T. *Macromolecules* **1987**, *20*, 1342–1344.

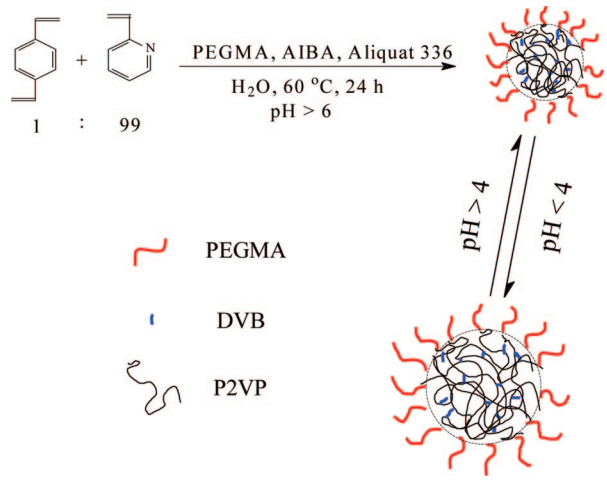

Figure 1. Schematic illustration of the synthesis of near-monodisperse, sterically stabilized poly(2-vinylpyridine) (P2VP) latex via emulsion polymerization at 60 °C, and the subsequent pH-induced swelling/deswelling of these particles in aqueous solution at 25 °C.

Table 1. Summary of Dynamic Light Scattering Data Obtained for Nonswollen and Swollen Poly(2-vinylpyridine) Particles at pH 10 (Latex) and 2 (Microgel)

entry no.	$<D_h>$ (nm) pH 2[a]	polydispersity index	$<D_h>$ (nm) pH 10[a]	polydispersity index	swelling ratio[b]
1	1270	0.10	380	0.08	3.3
2	1460	0.08	480	0.06	3.0
3	1650	0.13	560	0.09	2.9
4	1960	0.08	640	0.02	3.1
5	3120	0.10	830	0.08	3.8
6	4230	0.09	1010	0.09	4.2

[a] Intensity-average hydrodynamic diameters, $<D_h>$, and polydispersity indices, μ_2/Γ^2, were determined by dynamic light scattering at 25 °C. [b] Calculated from the ratio of the $<D_h>$ determined at pH 2 to that obtained at pH 10.

light scattering detector. These P2VP microgels were synthesized by emulsion copolymerization of 2VP with poly(ethylene glycol) monomethacrylate (PEGMA) at 60 °C using 1.0% divinylbenzene cross-linker. The grafted PEGMA chains located at the particle surface confer steric stabilization and hence prevent significant aggregation of the deswollen latex particles. The microgel-to-latex deswelling transition was actuated by a pH-jump from pH 2.0 to various final solution pH values. We then investigated the effects of final pH, salt concentration, and microgel dimensions on the kinetics of microgel deswelling. Diffusion coefficients were determined from the slope of the linear correlation between the characteristic deswelling time, $\tau_{deswell}$, and the square of the initial microgel radius, R^2.

Experimental Section

Sample Preparation. Synthetic protocols for the preparation of a series of near-monodisperse P2VP microgels have been previously described in detail.[3,4] A schematic representation outlining their synthesis is shown in Figure 1 and the physical parameters of these particles are summarized in Table 1. After extensive dialysis at pH 2 (MW cutoff ~14 000 Da) for three days, P2VP microgels were further diluted for subsequent stopped-flow kinetic studies.

Characterization. *Potentiometric Titrations.* The 640 nm P2VP latex particles were dispersed in deionized water at pH 10. The dispersion was titrated by the dropwise addition of 0.1 M HCl and the solution pH was monitored with a Corning Check-Mite pH meter (precalibrated with pH 4.0, 7.0, and 10.0 buffer solutions).

Laser Light Scattering (LLS). Intensity-average hydrodynamic diameters were measured at 25 °C using a Malvern Zetasizer ZEN 3600 instrument equipped with a 4 mW He−Ne solid-state laser operating at 633 nm. Back-scattered light was detected at 173° and the mean particle diameter was calculated from the quadratic fitting of the correlation function over 30 runs of 10 s duration. All measurements were performed in triplicate on highly dilute (0.01 w/v %) dispersions and analyzed using the Stokes−Einstein equation, which is valid for dilute, spherical, noninteracting particles.[3,4]

Stopped-Flow with Light-Scattering Detection. Stopped-flow studies were conducted using a Bio-Logic SFM300/S stopped-flow instrument equipped with three 10 mL step-motor-driven syringes (S1, S2, and S3), which can be operated independently to carry out single- or double-mixing. This stopped-flow device was attached to a MOS-250 spectrometer and kinetic data were fitted using the Biokine program provided by Bio-Logic. For light scattering detection at a scattering angle of 90°, both the excitation and emission wavelengths were adjusted to 335 nm with 10 nm slits. Using either FC-08 or FC-15 flow cells, typical dead times are 1.1 and 2.6 ms, respectively. The solution temperature was maintained at 25 °C by circulating water around the syringe chamber and observation head. Prior to loading into the motor-driven syringes, all aqueous solutions were clarified by passing through 2.0 μm Millipore Nylon filters. For pH jump experiments, the final pH was controlled by varying the mixing ratio of the P2VP latex dispersion (pH 2) to that of alkaline solution. The mixing ratios were calculated based on titration results, and the final pH after stopped-flow mixing was monitored with a Corning Check-Mite pH meter.

Results and Discussion

pH-Induced Volume Phase Transitions. The conjugated acid of linear P2VP homopolymer possesses a pK_a of 4.92 in dilute aqueous solution.[4] Below this critical value, linear P2VP is soluble as a weak cationic polyelectrolyte due to protonation of its pendent pyridine groups. For lightly cross-linked P2VP particles, Dupin et al.[4] reported that the apparent pK_a decreased approximately linearly with an increasing degree of cross-linking. For example, addition of 2.0 wt % DVB cross-linker to the emulsion polymerization of 2VP lowered the pK_a of the resulting particles from 4.75 to 3.85.

A typical acid titration curve for one of the P2VP latexes (entry 4 in Table 1) used in this study is shown in Figure 2a. Addition of 0.1 M HCl to this aqueous latex, initially at pH 10, leads to the onset of protonation of 2VP residues at pH 5.24, a strong buffer effect in the pH range of 3−5, and full protonation at pH 2.95. Using these titration data, we calculate that the overall degree of protonation of 2VP residues decreases from unity to zero as the solution pH increases from 2.95 to 5.24, see Figure 2b. Thus, the pK_a of the P2VP microgel with 1.0% DVB is determined to be 4.1, which is lower than that of the linear P2VP homopolymer. In this context, similar results were also reported for polyacids with increasing local chain segment densities. Plamper et al.[51] synthesized star-shaped poly(acrylic acid) and found that the apparent pK_a values shifted to higher values with increasing number of arms.

Intensity-average hydrodynamic diameters, $<D_h>$, and polydispersity indexes, μ_2/Γ^2, were determined by DLS (see Table 1) at 25 °C for a series of six lightly cross-linked (1.0% DVB) P2VP particles at pH 10 (nonswollen latex) and 2 (swollen microgel). In alkaline solution all latex dispersions exhibited monomodal size distributions and relatively narrow polydispersities ($\mu_2/\Gamma^2 < 0.13$). On adjusting to pH 2, complete protonation and extensive microgel swelling occurred. Swelling ratios, expressed as the $<D_h>$ at pH 2 to that at pH 10, are also summarized in Table 1. Thus, acid-induced swelling leads to a 2.9−4.2-fold increase in the linear dimension, depending on the initial latex diameter. It should be noted that the DLS data may not be very reliable for the two largest microgels, since their

(51) Plamper, F. A.; Becker, H.; Lanzendorfer, M.; Patel, M.; Wittemann, A.; Ballauf, M.; Muller, A. H. E. *Macromol. Chem. Phys.* **2005**, *206*, 1813–1825.

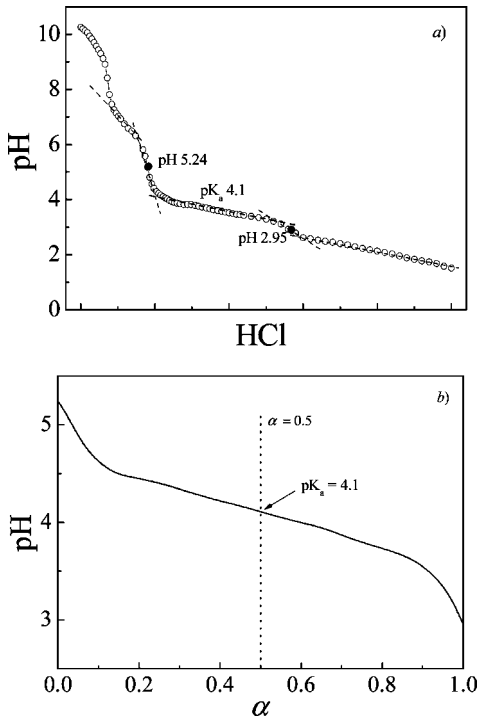

Figure 2. (a) Acid titration curve obtained for a 0.2 g/L aqueous solution of 640 nm P2VP latex (entry 4 in Table 1) in water using 0.1 M HCl. (b) Same titration curve as that shown in (a), with the *x*-axis expressed in terms of the mean degree of protonation, α.

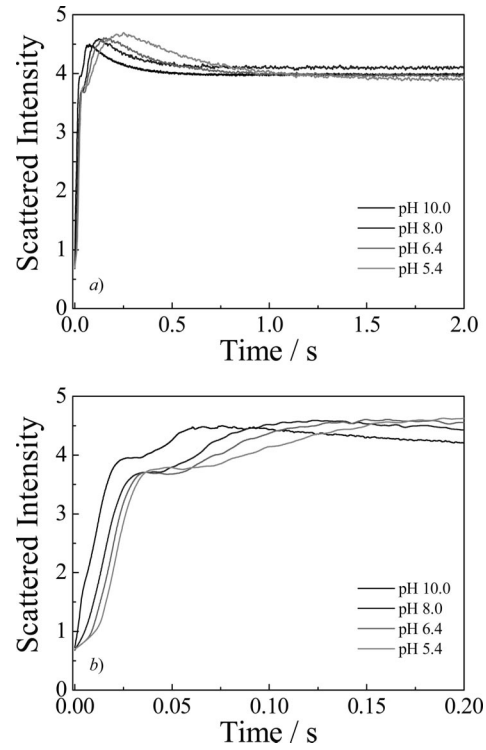

Figure 3. Variation in scattered light intensity for (a) long time scales and (b) short time scales for 1960 nm microgel (see entry 4 in Table 1) deswelling after a stopped-flow pH jump from 2 to various final pH values. The final microgel concentration was fixed at 4×10^{-6} g/mL.

swollen diameters lie close to the upper limit for this technique.

Final pH-Dependence of Microgel Deswelling Kinetics. In all previous studies concerning microgel swelling, the kinetics were simply monitored by following time-dependent changes of transmittance or absorbance after either a temperature or pH jump.[3,4,12,33,37] Thus particle concentrations were relatively high (0.1−3.0 g/L) to provide sufficient sensitivity. In principle, the scattered light intensity should be a much more sensitive method for monitoring the VPT. Since the particle concentration can be much lower, the volume change is more likely to reflect isolated (rather than interacting) microgel particles. Furthermore, changes in transmittance or absorbance can be sometimes complicated by particle flocculation or aggregation, especially at relatively high concentrations. Various techniques such as NMR, fluorescence, and small-angle neutron scattering (SANS) have suggested that there is a radial gradient of cross-linking density within microgels.[34,52–54] Thus, it is quite possible that, prior to the complete collapse of individual PNIPAM particles, interparticle aggregation may occur due to interactions between partially collapsed microgels. For these reasons, we have used a scattered light detector in preference to a transmitted light detector in the present study.

For all the microgel deswelling kinetic studies in this work, the final particle concentrations were fixed at 4×10^{-6} g/mL. Since this concentration is relatively low, all dispersions appear transparent over the whole pH range, i.e., visual inspection does not reveal any obvious changes in optical transmittance upon microgel deswelling. In situ deprotonation lowers the cationic charge density; hence the internal osmotic pressure within initially swollen microgels decreases. This will dramatically weaken the repulsive forces between neighboring chains and lead to collapse of the microgel network. The deswelling kinetics for the microgel-to-latex transition after a stopped-flow pH jump from 2 to various final pH values was then investigated.

Typical dynamic traces associated with the deswelling of 1960 nm P2VP microgels (initially at pH 2) are shown in Figure 3. For a pH jump from 2 to a final pH ≥ 5.4, microgel particles undergo complete deswelling, and the scattered light intensity typically exhibits an abrupt initial increase, and then stabilizes (Figure 3a). The whole deswelling process takes ∼0.5−1.0 s, which is much slower than the tens of milliseconds time scale reported for the kinetics of swelling of the same particles.[3,4] Similarly, Shibayama et al.[43,49] reported that the rate of gel deswelling was strongly retarded compared to that of gel swelling for macroscopic PNIPAM gels.

Based on the principles proposed by Tanaka[40] for macroscopic gels, we interpret our data as follows. Deprotonation of the microgel *exterior* occurs first, which leads to the formation of a collapsed, relatively dense outer shell and an abrupt increase in scattered light intensity. This initial fast process is followed by deprotonation of the swollen inner cores and the relatively diffusion of both water and salt (NaCl is formed due to the in situ acid−base neutralization) out of the shrinking microgels. The overall kinetics of deswelling will be retarded by the presence of the initially formed dense surface layer, which is impermeable to the inner fluid and suppresses the excretion of water and salt from the collapsing particle interior.

The change in scattered light intensity at 90° includes two opposing contributions: (i) the shrinking microgels cause an increase in scattered intensity due to their higher refractive index difference relative to water; (ii) deprotonation reduces the overall mass of P2VP particles due to excretion of NaCl and water, leading to a reduction in scattered intensity. Thus, the initial

(52) Annaka, M.; Tanaka, C.; Nakahira, T.; Sugiyama, M.; Aoyagi, T.; Okano, T. *Macromolecules* **2002**, *35*, 8173–8179.
(53) Shibayama, M. *Macromol. Chem. Phys.* **1998**, *199*, 1–30.
(54) Sugiyama, M.; Annaka, M.; Motokawa, R.; Kuwajima, S.; Hara, K. *Physica B* **2002**, *311*, 90–94.

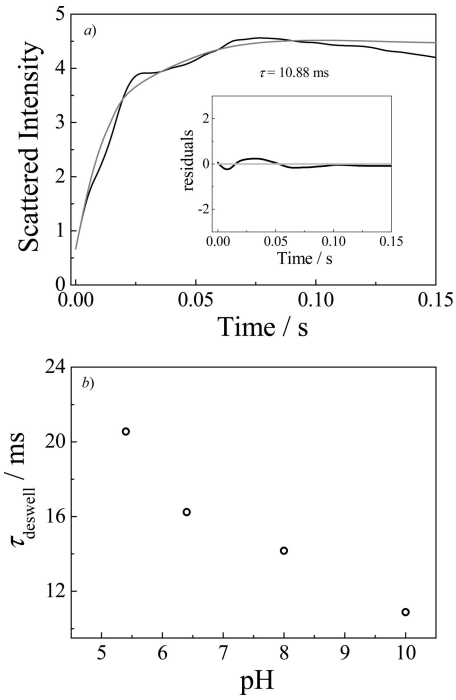

Figure 4. (a) Single exponential fitting of the dynamic traces obtained after a stopped-flow pH jump from 2 to 10. (b) Effect of solution pH on the characteristic deswelling time, $\tau_{deswell}$, of a 1960 nm poly(2-vinylpyridine) microgel after a stopped-flow pH jump from 2 to various final solution pH values. The experimental conditions were the same as those described in Figure 3b.

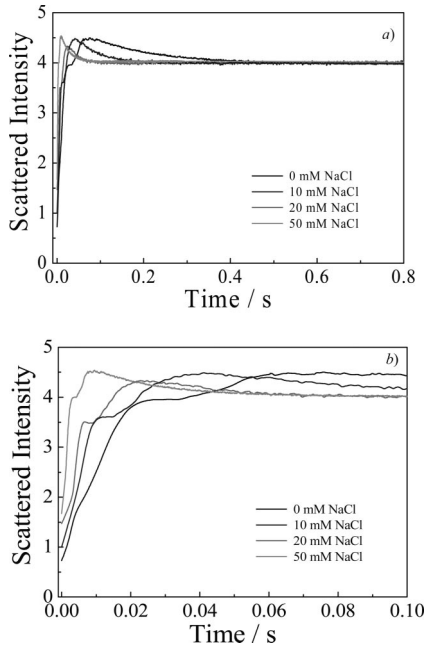

Figure 5. Variation in scattered light intensity for (a) long time scales and (b) short time scales observed for a deswelling 1960 nm microgel after a stopped-flow pH jump from 2 to 10 in the presence of different NaCl concentrations. The final microgel concentration was fixed at 4 $\times$ 10^{-6} g/mL.

increase in scattered light intensity during deswelling indicates that microgel shrinking dominates initially, while the subsequent gradual decrease in scattered light intensity strongly suggests that the diffusion of small molecules out of the microgel dominates over longer time scales. It is emphasized that such subtle details cannot be elucidated using a transmitted light detector.

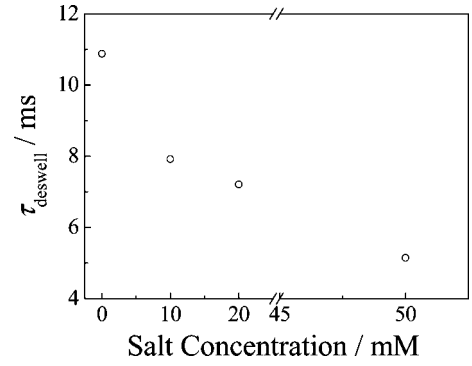

Figure 6. Salt concentration dependence of the characteristic deswelling time, $\tau_{deswell}$, obtained for initial deswelling of 1960 nm microgel after a stopped-flow pH jump from 2 to 10. The experimental conditions were the same as those described in Figure 5b.

Lyon and co-workers[12] examined the temperature-induced deswelling of PNIPAM microgels using a laser flash temperature-jump technique. A relatively short relaxation time of the order of μs was observed. Although a temperature jump of 10 °C was achieved within 20 ns, there was a delay time of 600 ns between the heating pulse and the onset of changes in transmittance. Moreover, only partial microgel shrinking was achieved and the deswelling transition resulted in a relatively modest reduction (<10%) in particle volume. Thus this experiment differs significantly from the current study in which extensive microgel shrinking was achieved.

Over relatively short time scales (0−0.2 s) (see Figure 3b), a dramatic increase in scattered light intensity occurs within the first ~50 ms, with a local plateau being observed thereafter. This local plateau regime is quite comparable to the intermediate plateau regime observed for macroscopic PNIPAM gels.[40] According to light scattering theory, the initial abrupt increase in scattered intensity indicates rapid shrinking of swollen microgels.[34,55,56] Single exponential fits to the dynamic traces at short time scales (0−0.2 s) are shown in Figure 4. On increasing the final pH from 5.4 to 10, the characteristic relaxation time for the initial microgel deswelling, $\tau_{deswell}$, ranges from 10 to 20 ms and decreases at higher final pH values. In other words, a larger pH jump leads to faster initial microgel deswelling. Similar observations were reported by Shibayama et al.[43] for macroscopic PNIPAM gels, which shrank faster at higher target temperatures.

Nevertheless, the rate of initial microgel deswelling is somewhat slower than that of the latex-to-microgel swelling process, as reported by Dupin et al.[3] According to the Tanaka equation (eq 1), this is expected in view of the differences between the initial swollen microgel diameter at pH 2 (1960 nm) and the nonswollen latex at pH 10 (640 nm), respectively (see Table 1). Given the R^2 dependence in the Tanaka equation, it is reasonable to observe that the former particles will respond over significantly longer time scales.

Effect of Salt Concentration on the Kinetics of Microgel Deswelling. Recent studies by Snowden et al.[57] and Nazbar et al.[58] indicate that the addition of NaCl can cause shrinking of PNIPAM microgels and PS/PNIPAM core−shell particles. Dupin and co-workers[3] studied the swelling kinetics of P2VP latex in the presence of NaCl and reported that added salt can significantly

(55) Chu, B. *Laser Light Scattering*; Academic Press: New York, 1991.
(56) Huglin, M. B. *Light scattering from polymer solutions*; Academic Press: New York, 1972.
(57) Snowden, M. J.; Vincent, B. *J. Chem. Soc. Chem. Commun.* **1992**, 1103–1105.
(58) Nabzar, L.; Duracher, D.; Elaissari, A.; Chauveteau, G.; Pichot, C. *Langmuir* **1998**, *14*, 5062–5069.

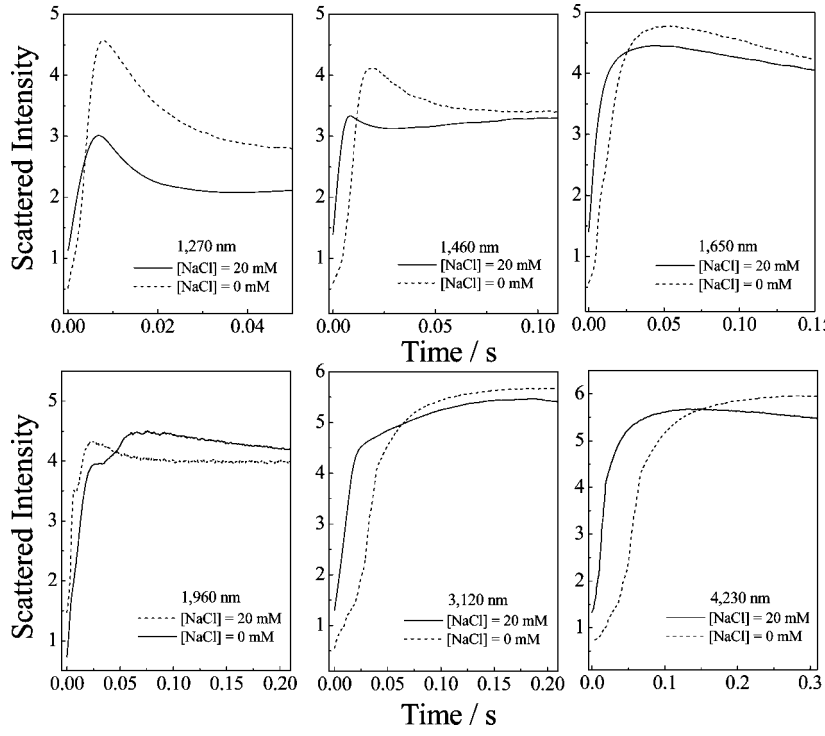

Figure 7. Comparison of time-dependent scattered light intensity curves obtained during the initial deswelling of six near-monodisperse poly(2-vinylpyridine) microgels (see entries 1−6 in Table 1) after stopped-flow pH jumps from 2 to 10 in the absence of salt and in the presence of 20 mM NaCl, respectively. The final microgel concentration was fixed at 4×10^{-6} g/mL.

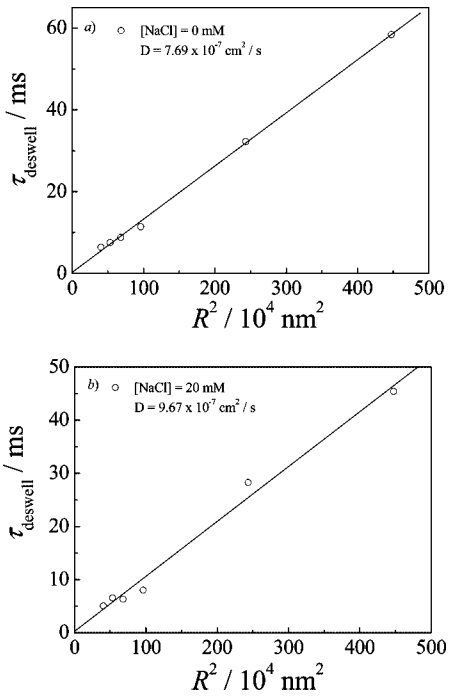

Figure 8. Correlation between the characteristic initial microgel deswelling time, $\tau_{deswell}$, and the square of the poly(2-vinylpyridine) microgel radius, R^2, obtained for a pH jump from 2 to 10 using six microgels of varying diameter (see entries 1−6 in Table 1): (a) in the absence of NaCl, and (b) in the presence of 20 mM NaCl.

enhance the swelling rates. Here we further examine the effect of added salt on the kinetics of deswelling of P2VP microgel particles of 1960 nm diameter (see entry 4 in Table 1).

Figure 5a and b shows the time-dependence of the scattered light intensity for both long and short time scales after a pH jump from 2 to 10 in the presence of various NaCl concentrations. In all cases, the scattered light intensity initially increases abruptly, followed by a slow gradual decrease. Apparently, the presence of increasing salt (0−50 mM) accelerates both the initial rapid microgel deswelling that occurs within the first 50 ms and also the subsequent equilibration processes. Single-exponential fits to these dynamic traces (Figure 5b) for the initial microgel deswelling are shown in Figure 6. As the concentration of added NaCl is increased from 0 to 50 mM, $\tau_{deswell}$ decreases from 11 to 5 ms.

On the other hand, separate DLS studies reveal that the average cationic P2VP microgel diameter at pH 2 decreases from 1960 to 1880 nm due to electrostatic screening as the NaCl concentration increases from 0 to 20 mM, whereas its particle size at pH 10 barely changes with added salt. The faster rate of initial microgel deswelling in the presence of added salt can thus be partially ascribed to differences in the microgel dimensions according to the Tanaka equation (eq 1).[45] Moreover, in the Tanaka equation (eq 1),[45] the collective diffusion coefficient (D) was defined as the osmotic bulk modulus (K) divided by the friction coefficient (f) between the gel network and the liquid. The presence of NaCl might lead to an increase in D and consequently a smaller $\tau_{deswell}$. An increase in the value of D will be confirmed in the following section.

The presence of increasing levels of background salt can also significantly reduce the time required for equilibration of the additional NaCl generated locally within the P2VP particles. This explains why the rate of microgel deswelling in the latter stage is faster in the presence of increasing NaCl concentration (see Figure 5a).

Microgel Size Dependence on the Deswelling Kinetics. At pH 2, the microgels are completely protonated and fully swollen. After a pH jump from 2 to a final pH ≥ 5.4, microgel particles undergo complete deswelling (see Figure 2). Using the same protocol developed for the 1960 nm diameter P2VP microgel, the deswelling kinetics of the microgel-to-latex transitions for

the other five P2VP microgels (diameters ranging from 1270 to 4230 nm, see Table 1) were investigated both in the absence and presence of NaCl.

In the absence of added salt, the time-dependent scattered light intensity curves obtained for all six microgels during their initial rapid deswelling phase is shown in Figure 7. In each case the scattered light intensity abruptly increases with time initially and then reaches a local plateau. In particular, slower rates of deswelling are observed for larger P2VP microgels. Given the differences in the initial particle dimensions prior to deswelling at pH 2, this behavior can be readily explained by considering the Tanaka equation. For example, if the initial microgel diameter is 4230 nm, the calculated $\tau_{deswell}$ is ~447 ms, which is much larger than that calculated for the 1270 nm microgel particles ($\tau_{deswell} \approx 40$ ms). It is noteworthy that smaller microgels respond faster in terms of both the initial microgel deswelling and also the subsequent slow equilibration process.

All the dynamic traces shown in Figure 7 for pH jumps conducted in the absence of salt can be well-fitted by single exponential functions. The characteristic deswelling time, $\tau_{deswell}$, ranges from 6 to 58 ms when the initial microgel diameter increases from 1270 to 4230 nm. Moreover, the near-linear correlation between $\tau_{deswell}$ and the square of the initial microgel radius, R^2, can be clearly seen in Figure 8a, which is in good agreement with the Tanaka equation[45] and also with the results reported by Dupin et al.[3] On the basis of eq 1, the collective diffusion coefficient, D, obtained for the initial microgel deswelling process in the absence of NaCl is calculated to be 7.7×10^{-7} cm^2 s^{-1} from Figure 8a. This value is in reasonable agreement with those D values determined for macroscopic gels by DLS (~5×10^{-7} cm^2 s^{-1}).[38,44] Analysis of the $\tau - R^2$ curve reported by Dupin et al.[3] for the microgel swelling process revealed a D value of ~1.5×10^{-7} cm^2 s^{-1}, which is quite comparable to that calculated for the microgel deswelling process.

The effect of added salt on the initial deswelling of the six microgels is also shown in Figure 7. Faster initial deswelling occurs in each case in the presence of 20 mM NaCl. The characteristic deswelling times, $\tau_{deswell}$, deduced from single exponential fitting are again plotted against the square of the microgel radius, and again a linear correlation is clearly evident (Figure 8b). The slope of the $\tau_{deswell} - R^2$ plot leads to a collective diffusion coefficient, D, of 9.7×10^{-7} cm^2 s^{-1} for microgel deswelling in the presence of 20 mM NaCl. Although the D values determined in the presence and absence of NaCl are comparable, the latter is slightly larger, possibly because the presence of background salt leads to a more compact microgel network initially. On the other hand, the larger D value observed in the presence of NaCl is fully consistent with the faster rate of microgel deswelling obtained under these conditions.

Conclusions

In summary, the pH-induced deswelling kinetics of sterically stabilized, micrometer-sized P2VP microgel particles in highly dilute aqueous solution (4×10^{-6} g/mL) was investigated using a stopped-flow light scattering technique. Complete deswelling within ~0.5−1 s was observed for a pH jump from 2 to above pH 5.4. However, this time scale is much slower than the kinetics of swelling recently reported for the same particles,[3] which occurred within tens of milliseconds. Reasonable explanations for the relatively slow rate of microgel deswelling are tentatively proposed. First, swollen microgels are much larger than non-swollen latex particles, and the characteristic time scales for both swelling and deswelling transitions depend on the particle size. Moreover, both a higher final pH and a greater external NaCl concentration leads to faster initial microgel collapse. For a series of six microgels of varying mean diameter, the characteristic time scale for *initial* deswelling, $\tau_{deswell}$, is closely correlated to the square of the microgel radius (R^2), as proposed for macroscopic gels by Tanaka's group[45] The calculated collective diffusion coefficient, D, deduced for the initial deswelling transition was estimated to be either 7.7×10^{-7} or 9.7×10^{-7} cm^2 s^{-1}, in the absence or presence of 20 mM NaCl, respectively. The larger D value in the presence of NaCl explains the faster deswelling rate of the microgel particles under these conditions.

Acknowledgment. The financial support of National Natural Scientific Foundation of China (NNSFC) Projects (20534020, 20674079, and 50425310), Specialized Research Fund for the Doctoral Program of Higher Education (SRFDP), and the Program for Changjiang Scholars and Innovative Research Team in University (PCSIRT) are gratefully acknowledged. SPA is the recipient of a five-year Royal Society-Wolfson Research Merit Award. D.D. thanks Rohm and Haas for funding his Ph.D. studentship.

LA8014282